

Disease's hidden death toll: Using parasite aggregation patterns to quantify landscape-level host mortality in a wildlife system

Mark Q. Wilber¹  | Cheryl J. Briggs¹  | Pieter T. J. Johnson² 

¹Ecology, Evolution and Marine Biology,
University of California, Santa Barbara,
Santa Barbara, CA, USA

²Ecology and Evolutionary Biology,
University of Colorado, Boulder, CO, USA

Correspondence

Mark Q. Wilber
Email: mark.wilber@lifesci.ucsb.edu

Funding information

National Institutes of Health, Grant/
Award Number: R01GM109499 and
R01GM135935; National Science
Foundation, Grant/Award Number: 1149308
1754171; National Geographic Society;
David and Lucile Packard Foundation

Handling Editor: Isabella Cattadori

Abstract

1. World-wide, infectious diseases represent a major source of mortality in humans and livestock. For wildlife populations, disease-induced mortality is likely even greater, but remains notoriously difficult to estimate—especially for endemic infections. Approaches for quantifying wildlife mortality due to endemic infections have historically been limited by an inability to directly observe wildlife mortality in nature.
2. Here we address a question that can rarely be answered for endemic pathogens of wildlife: what are the population- and landscape-level effects of infection on host mortality? We combined laboratory experiments, extensive field data and novel mathematical models to indirectly estimate the magnitude of mortality induced by an endemic, virulent trematode parasite (*Ribeiroia ondatrae*) on hundreds of amphibian populations spanning four native species.
3. We developed a flexible statistical model that uses patterns of aggregation in parasite abundance to infer host mortality. Our model improves on previous approaches for inferring host mortality from parasite abundance data by (i) relaxing restrictive assumptions on the timing of host mortality and sampling, (ii) placing all mortality inference within a Bayesian framework to better quantify uncertainty and (iii) accommodating data from laboratory experiments and field sampling to allow for estimates and comparisons of mortality within and among host populations.
4. Applying our approach to 301 amphibian populations, we found that trematode infection was associated with an average of between 13% and 40% population-level mortality. For three of the four amphibian species, our models predicted that some populations experienced >90% mortality due to infection, leading to mortality of thousands of amphibian larvae within a pond. At the landscape scale, the total number of amphibians predicted to succumb to infection was driven by a few high mortality sites, with fewer than 20% of sites contributing to greater than 80% of amphibian mortality on the landscape.
5. The mortality estimates in this study provide a rare glimpse into the magnitude of effects that endemic parasites can have on wildlife populations and our theoretical framework for indirectly inferring parasite-induced mortality can be applied to other host–parasite systems to help reveal the hidden death toll of pathogens on wildlife hosts.

KEYWORDS

aggregation, infectious disease, macroparasite, negative binomial, parasite-induced mortality, *Ribeiroia ondatrae*, virulence

1 | INTRODUCTION

World-wide, infectious diseases continue to be a major source of human mortality, killing an estimated 5 million people globally per year with a crude death rate of 76 per 100,000 persons (prior to the COVID-19 pandemic; World Health Organization, 2018). In wildlife populations, the amount of disease-induced mortality is likely even higher, yet obtaining accurate estimates of wild hosts killed by parasites and pathogens is notoriously difficult. Many of the most striking effects of disease on wildlife populations are when the introduction of a novel pathogen leads to epizootics and dramatic declines in host populations. For example, disease-induced population declines have been observed in amphibians due to chytridiomycosis (Scheele et al., 2019), bats suffering from white-nose syndrome (Blehert et al., 2008), Tasmanian devils with facial tumour disease (McCallum et al., 2009) and Siaga antelope experiencing haemorrhagic septicaemia (Fereidouni et al., 2019). What evidence is available also suggests that the burden of pathogens on wildlife is increasing (Fisher et al., 2012; Jones et al., 2008).

While such examples highlight the potential for novel or introduced diseases to induce mortality among hosts, even endemic infections likely represent an important—yet more difficult to quantify—cause of death in natural populations. Many well-established parasites cause substantial harm or even mortality in their hosts in the absence of epidemics. For example, strongyle nematode parasites that persist endemically in wild sheep populations decrease body weight and fecundity in adult sheep and increase overwinter mortality in juveniles (Hayward et al., 2019). Some parasites even depend on host death for transmission. For instance, 'obligate killer' parasites such as chytrid infections in *Daphnia*, fungal parasites of ants and parasitoid wasps can only spread or persist following the eventual death of the infected host (Johnson et al., 2006; Murdoch et al., 2005; Pontoppidan et al., 2009). Host death is also a necessary outcome for multi-host parasites that use trophic transmission. Many helminth parasites (e.g. species of trematodes, cestodes and nematodes), for example, depend on predation as a vehicle to move between their intermediate hosts (often an invertebrate) and a suitable definitive host (often a vertebrate predator, Lafferty & Kuris, 2002). Because sexual reproduction frequently occurs only in the definitive host, some trophically transmitted parasites induce physical or behavioural changes in intermediate hosts that enhance their susceptibility to predators (Poulin & Morand, 2000). The risk of predation among infected hosts may be 30x greater than within their uninfected conspecifics (Lafferty & Morris, 1996).

Quantifying the effects of parasites—including novel as well as endemic infections—on host populations is therefore critical for understanding overall wildlife health, yet methods for estimating these numbers and their uncertainty remain a persistent challenge (Scott, 1988; Tompkins et al., 2011, 2015). Estimating parasite-induced

mortality requires monitoring of host populations before and after declines or quantifying host carcasses, yet pathogen monitoring in wildlife populations is often initiated only after a pathogen has been identified as a threat. Moreover, inferring the cause of mortality from an observed carcass is fraught with difficulty (McCallum, 2000, 2012), and dead hosts often disappear rapidly from the environment prior to detection by observers. Effectively linking field-observed mortality to pathogen infection requires a combination of laboratory experiments demonstrating the effects of infection (Johnson et al., 2012), models linking the individual-level effects of parasitism to population effects (Dobson & Hudson, 1992; Krkošek et al., 2009) and field experiments to test these predictions (Hudson et al., 1998; Watson, 2013). Not surprisingly, studies that combine these three ingredients are rare, in part due to their logistical challenges (Tompkins et al., 2011). When not all of these ingredients can be fulfilled, a key question is under what conditions can we still infer parasite-induced mortality on wildlife hosts.

One intriguing approach for inferring the parasite-induced mortality involves the observed distribution of parasites within hosts (Crofton, 1971; Ferguson et al., 2011). Particularly for macroparasites, the distribution of parasite abundance within a host population almost universally follows a negative binomial distribution, in which the variance in infection exceeds the mean value (Shaw et al., 1998). Over-dispersion has been so consistently observed in macroparasite infections that it is referred to as one of the few 'laws' of parasitology (Poulin, 2007). Because heavily infected hosts are more likely to exhibit mortality (i.e. intensity-dependent pathology), parasite-induced mortality of hosts should ultimately remove a disproportionate fraction of heavily infected hosts, causing the distribution to become less aggregated (Figure 1, Crofton, 1971). For example, Ferguson et al. (2011) used truncation in macroparasite distributions to identify the threshold of parasite intensity above which Coho salmon suffer significant mortality. However, this approach has historically been limited in application both because (a) mechanisms other than parasite-induced mortality of hosts can also lead to reduced aggregation in host–parasite distributions (e.g. parasite competition, Barbour & Pugliese, 2000) and (b) it requires that infection and mortality occur prior to host sampling (Adjei et al., 1986), which clearly will not be true in all host–parasite systems. Moreover, using an observational approach often requires a large number of sampled hosts (e.g. >100, Wilber et al., 2016), which can be limiting when the goal is to compare mortality across multiple host populations.

In this study, we endeavour to overcome these limitations by combining novel theoretical models, laboratory infection experiments and an uniquely extensive field dataset (over 300 populations of four host species sampled across 6 years). Our goal was to use interactions between larval amphibian hosts and the pathogenic trematode, *Ribeiroia ondatrae*, to quantitatively estimate the amount

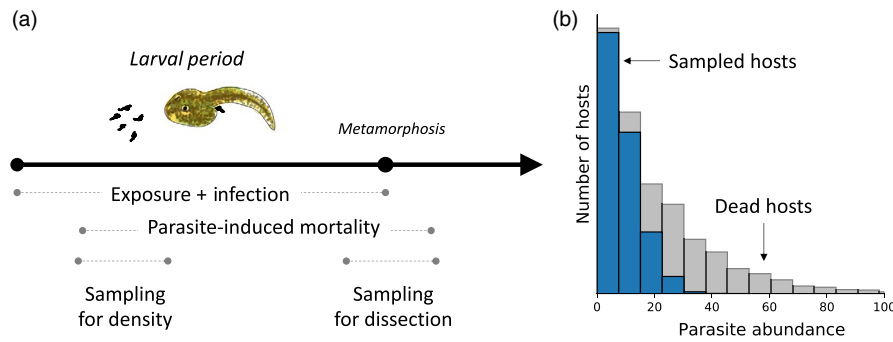


FIGURE 1 (a) To infer parasite-induced host mortality from observational data, the conceptual approach of Crofton (1971) assumes that sampling of hosts for dissection occurs after the majority of infection and parasite-induced mortality has occurred for a host. For the amphibian-*R. ondatrae* system considered in this study, amphibian larvae are only infected by *R. ondatrae* cercariae (black shapes) during their aquatic larval stage, where they also experience parasite-induced mortality. Hosts are sampled for dissection as late-stage larvae (caudates) or early metamorphs (anurans) after the infection period. In our study, host density was measured early in the summer, before the majority of parasite-induced mortality had occurred. (b) A graphical representation of how intensity-dependent parasite mortality can lead to truncation of the observed host–parasite distribution. The blue histogram shows the distribution of parasite abundances in sampled hosts and the gray histogram shows the distribution of parasite abundances in hosts that succumbed to parasite-induced mortality before sampling

of parasite-induced mortality among host populations, host species and through time. Specifically, we address a question that is rarely answerable for endemic pathogens of wildlife: what are the population- and landscape-level effects of this parasite on host mortality? Interactions between amphibian hosts and the trematode *R. ondatrae* offer a valuable system in which to address this question because they satisfy the assumptions necessary for inferring parasite-induced mortality (Figure 1). Infectious cercariae of *R. ondatrae* invade amphibians during their aquatic larval development period, such that parasite-induced mortality generally occurs prior to metamorphosis—the time in which hosts are typically sampled (Johnson & McKenzie, 2008; Johnson et al., 2016). Moreover, laboratory experiments with 12 amphibian species have shown that *R. ondatrae* causes dose-dependent mortality in larval amphibians, which is associated with corresponding reductions in aggregation (Johnson et al., 2012; Johnson & Wilber, 2017). This facilitates a novel opportunity to integrate extensive field surveys with detailed experimental results on the sensitivity of different host species to provide quantitative estimates of parasite-induced mortality in natural populations. Although our study does not assess the degree to which such mortality is additive or compensatory relative to other threats, it nonetheless offers an important insight into the heterogeneous effects of parasites across host populations and creates a template for estimating mortality in other host–parasite systems.

2 | MATERIALS AND METHODS

2.1 | Empirical data

2.1.1 | Field sampling

To characterize patterns of infection in wild-caught amphibians among species, across populations and through time, we sampled

7,689 amphibian hosts from 202 unique ponds (sites) in the East Bay region of California (Alameda, Contra Costa and Santa Clara counties) between 2009 and 2014 (dataset previously reported in Johnson et al., 2013, 2016). This included sites from publicly accessible parks, open space preserves, municipal watershed districts and private ranches. Each pond was visited twice within a year. During the first visit in late spring/early summer, we quantified the density of larval amphibians using dipnet surveys performed every 10m along the shoreline of each pond. All larvae captured within a dipnet sweep were identified and counted. A single dipnet sweep sampled approximately 0.5 m² (Richgels et al., 2013). The perimeter of each pond was measured using a hand-held GPS while walking the circumference. The number of unique sites sampled for host density each year were: 2009, $n = 77$; 2010, $n = 104$; 2011, $n = 72$; 2012, $n = 34$; 2013, $n = 80$ and 2014, $n = 56$.

The second visit in mid- to late-summer was timed to overlap with amphibian metamorphosis for parasitological sampling. We focused on recently metamorphosed amphibians, as these provide a reliable and standardized indicator of *R. ondatrae* infections acquired during aquatic development (Johnson et al., 2016). To measure *Ribeiroia* abundance per host, we performed a systematic examination of all major tissues and organs in sampled hosts (Hartson et al., 2011). In the analysis of parasite-induced mortality, we focused on the 301 site-by-year-by-host species combinations with at least five sampled hosts and five detected *R. ondatrae* metacercariae. This cut-off ensured sufficient statistical power to estimate the variance of the host–parasite distribution. These data included 173 populations (site-by-year combinations) of *Pseudacris regilla* (Pacific chorus frog, $n = 2,243$ individual hosts), 76 of *Taricha torosa* (California newt, $n = 868$ hosts), 39 of *Anaxyrus boreas* (western toad, $n = 526$ hosts) and 13 of *T. granulosa* (rough-skinned newt, $n = 139$ hosts). Table S1 describes how these populations were distributed across years.

2.1.2 | Laboratory experiments

We used controlled laboratory experiments to estimate the dose-response curves between *R. ondatrae* exposure and survival for larvae of the four amphibian species (Johnson & Wilber, 2017). We collected recently deposited amphibian egg masses (*P. regilla*, *A. boreas* and *T. torosa*) from field sites or reproductive adults (*T. granulosa*) and allowed them to lay eggs in the laboratory. Hatching larvae were maintained in carbon-filtered, UV-sterilized tap water at 22°C until being assigned randomly to one of five exposure dosages (0 [control], 20, 40, 100 or 200 cercariae). Snails *Helisoma trivolvis* naturally infected with *R. ondatrae* were collected from field sites, isolated into 50 ml vials and allowed to release free-swimming cercariae that were harvested within 4 hr of emergence (see Johnson et al., 2012). Pooled cercariae from multiple snails were administered to an individual amphibian larva within 500 ml of water. Larval amphibians were exposed to cercariae in a single pulse event timed to correspond to early limb development (anurans stage 28, caudates stage 2T; Gosner, 1960; Wong & Liversage, 2005). After exposure, we monitored amphibian larvae until death or 20 days following exposure, at which point we dissected hosts to quantify infection.

Cercariae of *R. ondatrae* are generally highly successful in finding and penetrating amphibian larvae within the small volumes of water we used in the experiment. However, not all parasites persisted within the host after 20 days, and we calculated the per cent of successful infections relative to parasites administered as a measure of host species competence (Johnson & Wilber, 2017). Previous studies have shown that the percentage of parasites persisting is independent of exposure dose (Johnson & Hoverman, 2012; Johnson & Wilber, 2017); we therefore assumed that, for any hosts that suffered parasite-induced mortality in the experiments, their infection load at the time of death was equal to their exposure dose multiplied by the empirically estimated competence value. We then used a survival analysis framework to estimate an intensity-dependent hazard function $\alpha(x)$ for each host species (details in Appendix S1), which describes the instantaneous host mortality rate given a parasite intensity of x .

2.2 | Estimating parasite-induced mortality

For a host-macroparasite system such as amphibian hosts and the trematode *R. ondatrae*, sampling of hosts primarily occurs after infection and parasite-induced mortality (Figure 1). Larval amphibians accumulate water-borne trematode cercariae during their aquatic development; those individuals surviving to metamorphosis no longer acquire new infections once they leave the water. Thus, parasite abundance within a sampled host is conditional on surviving parasite-induced mortality during the larval period of parasite exposure. Specifically, we can describe the probability of parasite abundance x on a sampled host $[x|\text{survival}]$ using the conditional probability (Wilber et al., 2016).

$$[x|\text{survival}] = \frac{[\text{survival}|x][x]}{[\text{survival}]} \quad (1)$$

$[\text{survival}|x]$ gives the probability of a host surviving until sampling (here, metamorphosis), given a parasite abundance of x at sampling. $[x]$ gives the probability of a host having a parasite abundance of x before mortality occurs. Finally, $[\text{survival}] = \sum_{x=0}^{\infty} [\text{survival}|x][x]$ gives the average survival probability of a host at sampling.

The functions in Equation 1 have strong empirical links to host-macroparasite systems. $[x]$ describes the population-level distribution of parasite abundances across hosts in the absence of parasite-induced mortality. Consistent with many empirical host-macroparasite distributions (Shaw et al., 1998), we let $[x]$ be described by a negative binomial distribution $[x] = g(x; \mu, k) = \frac{\Gamma(k+x)}{\Gamma(k)\Gamma(x+1)} \left(\frac{k}{k+\mu}\right)^k \left(\frac{\mu}{k+\mu}\right)^x$. The parameter μ describes the mean parasite intensity before mortality, the parameter k is an inverse measure of parasite aggregation before mortality (smaller k is more aggregated), and $\Gamma(\cdot)$ is the gamma function.

The probability $[\text{survival}|x]$ describes a dose-response curve between parasite abundance and host survival until sampling. Phenomenologically, $[\text{survival}|x]$ could be assumed to follow a standard dose-response curve such as a logistic curve (Wilber et al., 2016). More mechanistically, this function will depend on the underlying intensity-dependent hazard function $\alpha(x)$ as well as how parasites accumulate in hosts before sampling (during the larval period in this study). Instead of inferring $[\text{survival}|x]$ directly from field data, we estimated the intensity-dependent hazard function $\alpha(x)$ from laboratory data. We then assumed that parasites accumulated in hosts linearly over the larval period and estimated $[\text{survival}|x] = h(x; a, b, T_E)$ for each host species in the field (see Appendix S1 for details and justification). The parameter a is the parasite intensity at which a change in parasite intensity leads to the largest change in host mortality rate and b is an inverse measure of how much host mortality rate increases with increasing parasite intensity at a . T_E is a known parameter that gives the average length of the larval period in days for a host species. For this analysis, we used larval periods of 37 days for *A. boreas*, 60 days for *P. regilla* and 75 days for *T. torosa* and *T. granulosa* (AmphibiaWeb, 2020).

Given $[x] = g(x; \mu, k)$ and $[\text{survival}|x] = h(x; a, b, T_E)$, we can compute the average probability that a host suffered parasite-induced mortality

$$\Omega = 1 - \sum_{x=0}^{\infty} \frac{h(x; a, b, T_E)}{h(0; a, b, T_E)} g(x; \mu, k) \quad (2)$$

The derived parameter Ω estimates the impact of a parasite on a host population. Note that Equation 2 is conditional on a host surviving until sampling when parasite abundance is zero. Therefore, this estimate ignores the costs of preventing parasite infection through resistance mechanisms (Sears et al., 2015), which can also affect survival even in the absence of infection. We would therefore expect estimates of Ω to provide a lower bound on parasite-induced mortality in a host population.

2.3 | Statistical model for parasite-induced mortality

In practice, uniquely estimating all four parameters a , b , μ and k used in Equation 2 from field data alone requires at least 100 sampled hosts (Wilber et al., 2016). However, we were in the unique position in that we had laboratory data to infer the survival probability [survival|x] = $h(x; a, b, T_E)$ and could then use the field data to make inference on μ and k .

As described in Appendix S1, we estimated [survival|x] = $h(x; a, b, T_E)$ for each of the four amphibian species using the aforementioned laboratory experiments. For each amphibian species, we then estimated parasite intensity before mortality μ and parasite aggregation before mortality k for site m in year n . We modelled the probability of observing parasite abundance $x_{j,m,n}$ on host j in site m in year n as

$$[x_{j,m,n}] = \phi_{m,n} g(x_{j,m,n}; \mu_{m,n}, k_{m,n}) + (1 - \phi_{m,n}) \frac{h(x_{j,m,n}; a, b, T_E) g(x_{j,m,n}; \mu_{m,n}, k_{m,n})}{\sum_{i=0}^{\infty} h(i; a, b, T_E) g(i; \mu_{m,n}, k_{m,n})}, \quad (3)$$

$$\log(\mu_{m,n}) = \beta_n + \alpha_{m,n},$$

$$\log(k_{m,n}) = \omega_n + \gamma_{m,n}.$$

Equation 3 included fixed effects (β_n) of year on pre-mortality parasite intensity $\mu_{m,n}$, fixed effects (ω_n) of year on aggregation $k_{m,n}$ and random effects of site m in year n on parasite intensity ($\alpha_{m,n}$) and aggregation ($\gamma_{m,n}$). We also included a parameter $\phi_{m,n}$ that gave the probability that a host was sampled before it would have succumbed to mortality. This parameter allowed us to relax the assumption that all parasite-induced mortality occurred before sampling and generally improved the fit of our models to data (Figure S1). Given the assumption that parasites are distributed according to a negative binomial distribution before mortality, any source of host mortality that occurred independently of parasite intensity does not affect either mean parasite intensity or the aggregation parameter k and thus does not affect our ability to infer parasite-induced mortality (Pielou, 1969). We fit the above model in a Bayesian framework using PyMC3 with Hamiltonian Monte Carlo (details in Appendix S2, Salvatier et al., 2016). We assessed goodness-of-fit by comparing simulations of the model to observed data (Figure S1). We used the posterior distributions of $\mu_{m,n}$, $k_{m,n}$, a and b to compute population-level parasite-induced mortality $\Omega_{m,n}$ for site m in year n using Equation 2.

2.4 | Total parasite-induced mortality in host populations

For each site-by-year combination, we used our density estimates of amphibian larvae to calculate the total abundance of a species at site m in year n , $N_{m,n}$, by multiplying observed density by the area of the littoral zone of a pond. We approximated the area of the littoral zone

as pond perimeter \times 1 m. This approach assumes that larval amphibians are primarily concentrated in the shallow areas within 1 m of the shoreline, which is reasonable for the pond environments in our system. The median area of the littoral zone for the sampled ponds was c. 100 m². We then computed the number of larvae that suffered parasite-induced mortality at site m in year n for a given species as $D_{m,n} = N_{m,n} \Omega_{m,n}$. Our estimate of total mortality is consistent with larval density samples being taken early in the summer before substantial parasite-induced mortality had occurred (see Section 2.1.1, Figure 1a). If we instead assumed, for example, that density sampling occurred after mortality, our estimates of total mortality would be substantially higher. Thus, in addition to being consistent with our sampling design, assuming that density sampling occurred before mortality provided a conservative estimate of total parasite-induced mortality.

For sites where we had density data but did not dissect any hosts (638 site-by-year-by-host combinations), we estimated Ω as $\psi_n \Omega'$, where ψ_n was the observed occupancy probability of *R. ondatrae* across sites in year n (Table S2) and Ω' was the mean estimated parasite-induced mortality for a host species, pooled across years. We then calculated the total number of hosts suffering parasite-induced mortality as described above. For sites where we dissected hosts but the total number of observed parasites was less than five, we set Ω to zero to be conservative regarding parasite-induced mortality (399 site-by-year-by-host combinations, 308 where the total observed parasites was zero). We estimated the total number of larvae that suffered parasite-induced mortality on the landscape by summing total mortality $D_{m,n}$ across all sites sampled for host density within a given year and dividing by the total littoral area of the sites sampled.

3 | RESULTS

3.1 | Host competence and laboratory infections

Taricha torosa and *P. regilla* were the most competent host species (mean: 51%, 95% credible interval, CI: [47%, 55%]; mean 42%, 95% CI: [37%, 45%], respectively), where competence was defined as the percentage of total *R. ondatrae* cercariae that infected and persisted in a host 20 days post-exposure. *Taricha granulosa* and *A. boreas* were the least competent hosts (mean 27%, 95% CI: [23%, 31%]; mean 28%, 95% CI: [19%, 37%], respectively).

We combined these mean competence values with our experiment examining host survival to parasite exposure to estimate the rate of intensity-dependent amphibian mortality. We observed intensity-dependent amphibian mortality due to *R. ondatrae* in all four species of amphibians (Figure 2). Over 20 days, the median parasite intensity at which 50% of larvae were predicted to succumb to parasite-induced mortality was four parasites for *A. boreas* (95% CI: [3.08, 4.77]), 23 for *P. regilla* (95% CI: [16.5, 34.83]), 9 for *T. granulosa* (95% CI: [6.45, 12.9]) and 26 for *T. torosa* (95% CI: [19.23, 36.43]; Figure 2).

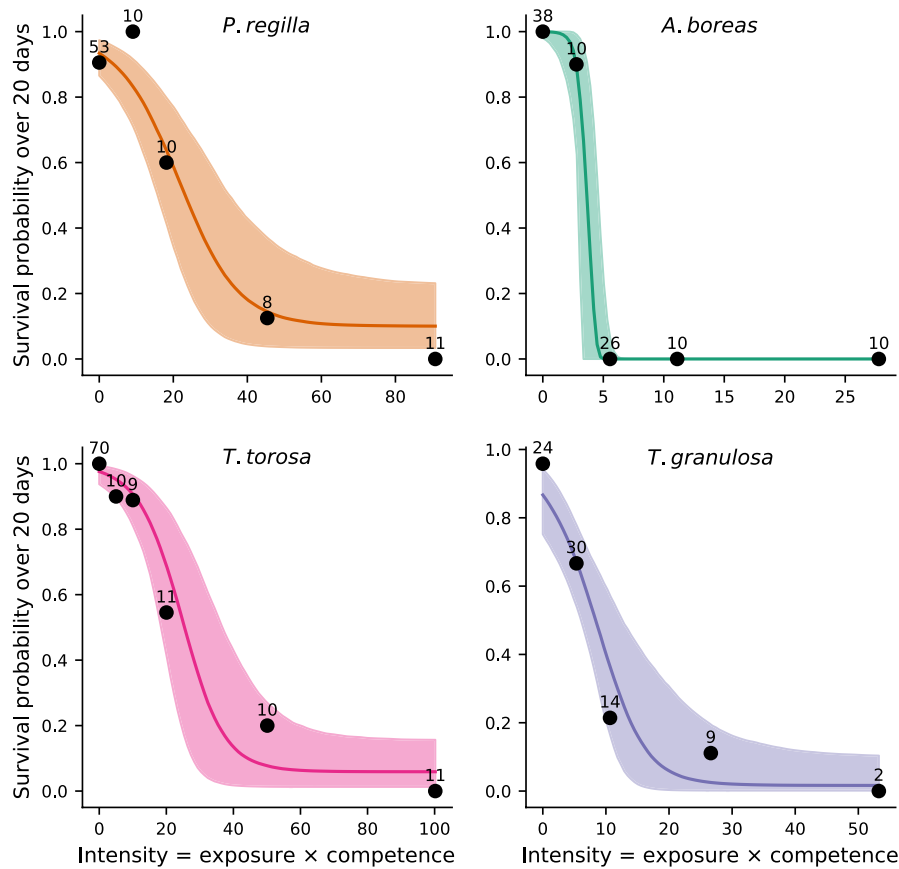


FIGURE 2 The host survival curves estimated from the laboratory experiment where four species of amphibian larvae were exposed to varying abundances of *R. ondatrae* cercariae and host survival was recorded after 20 days. To link the laboratory experiment to observed parasite intensity in the field, we calculated parasite intensity as exposure \times competence. Exposure was the number of cercariae to which a larva was exposed and competence was the average percentage of cercariae that successfully infected a host after 20 days. The black dots give the empirically observed host survival probability for the *R. ondatrae* intensity over 20 days. The numbers give the host sample size at each intensity. The colored lines give the best fit survival function over 20 days. The survival function is defined as $S(x|20 \text{ days}) = \exp(-\alpha(x) \times 20 \text{ days})$ where $\alpha(x)$ is the intensity-dependent hazard function at parasite intensity x . As described in Appendix S1, $\alpha(x)$ follows a logistic distribution and is defined as the instantaneous rate of host mortality given a parasite intensity of x . The shaded regions are the 95% credible intervals about the survival function

3.2 | Patterns of parasite infection and amphibian density in the field

In field surveys, *P. regilla* was the most wide-spread amphibian host with site-level mean occupancy $>70\%$ for all 6 years and $>90\%$ for 4 years (Figure 3a). *Taricha torosa* had the next highest occupancy, followed by *A. boreas* and *T. granulosa* (Figure 3a). Conditional on occupancy, *A. boreas* or *P. regilla* had the highest mean density per year, followed by *T. torosa* and then *T. granulosa* (Figure 3b).

Across years, *R. ondatrae* prevalence in dissected larvae was generally between 20% and 60% (Figure 3c). From 2011 to 2014 observed *R. ondatrae* prevalence in *A. boreas* was generally lower than *P. regilla* and *T. torosa* (Figure 3c). At sites where *R. ondatrae* was detected, mean infection intensity per larvae was generally less than 10 for all host species (Figure 3d), but could range as high as 25 for *T. granulosa*, 34 for *A. boreas*, 108 for *P. regilla* and 212 for *T. torosa* in some sites. Finally, *R. ondatrae* distributions for all host species were

aggregated, with variance in infection intensity being greater than mean infection intensity (Figure S2).

3.3 | Estimates of parasite-induced mortality in host populations

Across all years, *A. boreas* had the highest median population estimates of parasite-induced mortality (Ω), ranging from 23% to 48% (Figure 4a). However, due to the small within-year sample sizes there was large uncertainty around these yearly estimates (Figure 4a). Pooling across years, *A. boreas* had a median parasite-induced mortality of 39% (95% CI: [24.6%, 53.3%]), which was significantly or marginally significantly larger than the estimated parasite-induced mortality for *P. regilla* (median parasite-induced mortality for *P. regilla*: 14%, 95% CI: [9.8%, 19.8%]; 95% CI of difference in Ω between *A. boreas* and *P. regilla*: [9.2%, 39.7%]; Figure 4a), *T. torosa* (median parasite-induced mortality for *T. torosa*: 13.2%, 95% CI: [6.8%,

FIGURE 3 (a) The occupancy probability of hosts in sites over 6 years. (b) The density of amphibian larvae per dip net sweep ($\approx 0.5 \text{ m}^2$) given site occupancy. The number of sites sampled for host density in each year was: 2009, $n = 77$; 2010, $n = 104$; 2011, $n = 72$; 2012, $n = 34$; 2013, $n = 80$; 2014, $n = 56$. The sites for which we inferred parasite-induced mortality were a subset of these sites. (c) The observed prevalence of *R. ondatrae* in all dissected hosts within a given year for 6 years of sampling. (d) The observed infection intensity in dissected hosts for 6 years of sampling. For *T. torosa* in 2009, host density was sampled in $n = 77$ sites, but larvae were only dissected from two sites (Table S1)

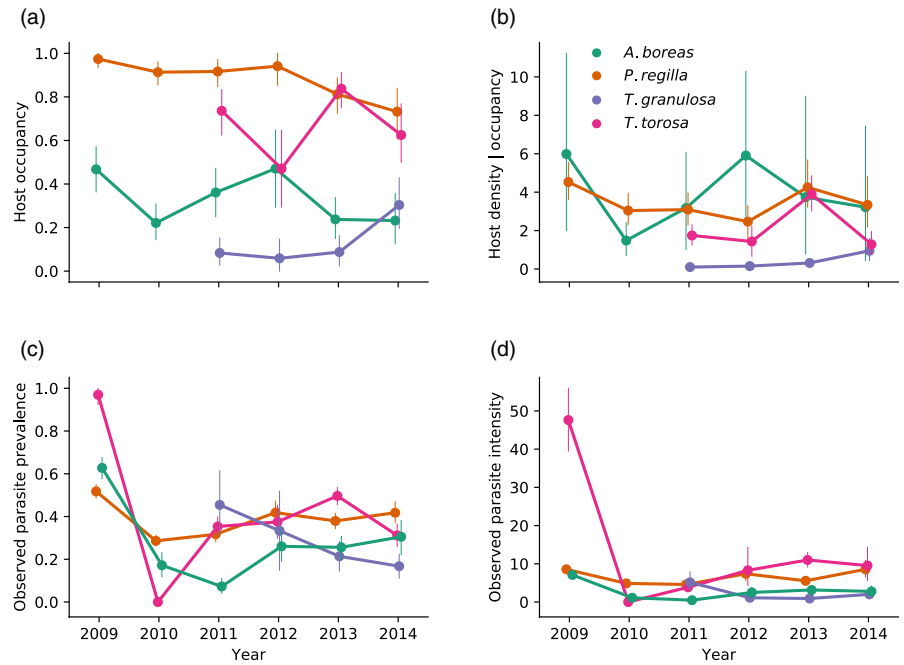
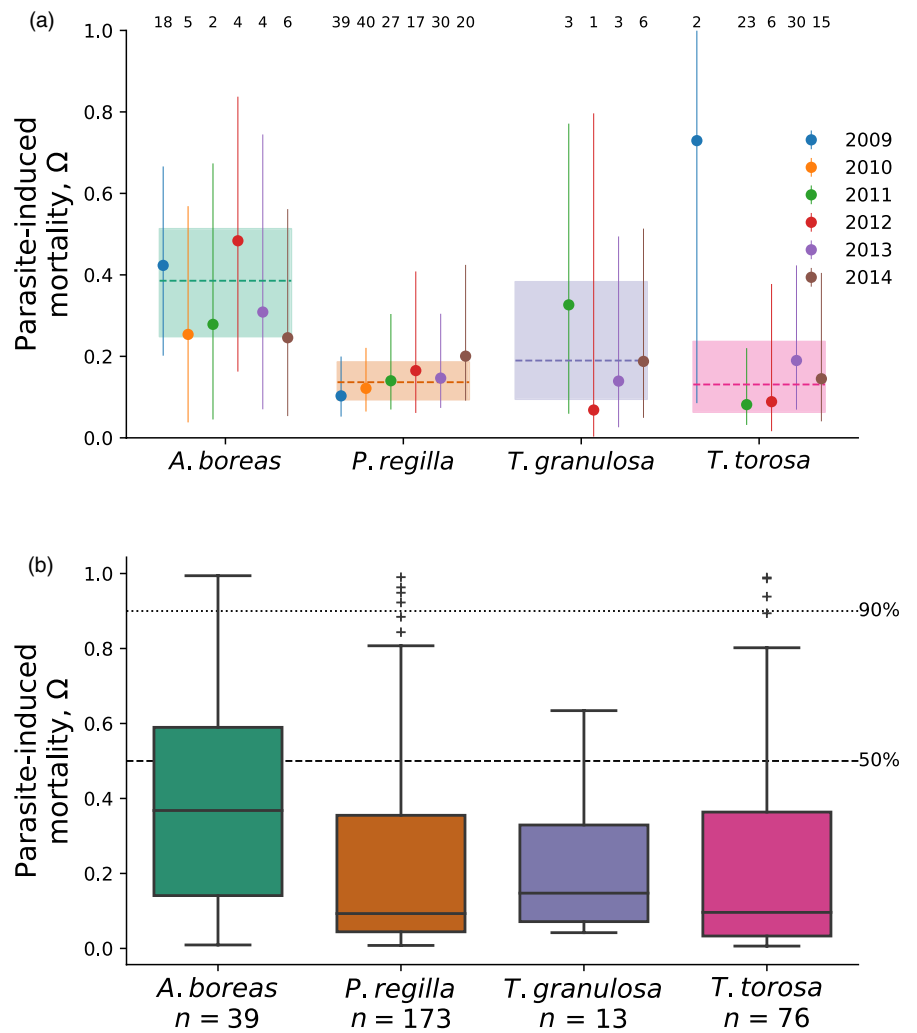


FIGURE 4 (a) The predicted population-level parasite-induced mortality (Ω) for four amphibian species. The coloured circles give the median estimated parasite-induced mortality by year and the numbers above each circle indicate how many populations of that species were used to infer the yearly, population-level estimate. The coloured rectangles given the 95% credible intervals for parasite-induced mortality estimates for a population, pooled across years. The dashed coloured lines are the median population-level mortality estimates, pooled across years. (b) Boxplots of the predicted site-level parasite-induced mortality (Ω) for the four amphibian species. Dashed and dotted lines show 50% parasite-induced mortality and 90% parasite-induced mortality respectively. Bars give the median parasite-induced mortality across sites, box edges give the first and third quartiles, and whiskers are the maximum point within 1.5 times of the inter-quartile range. Crosses are the observed parasite-induced mortality values that fall outside of the whiskers. The number of populations for each species is given on the x-axis. Site-level estimates of μ and k are Provided in Figure S3



23.2%]; 95% CI of difference in Ω between *A. boreas* and *T. torosa*: [8.4%, 40.6%]; Figure 4a) and *T. granulosa* (median parasite-induced mortality for *T. granulosa*: 18.5%, 95% CI: [8.1%, 36.5%]; 95% CI of difference in Ω between *A. boreas* and *T. granulosa*: [-3.3%, 38.6%]; Figure 4a).

There were 20 species-by-site-by-year combinations where inferred median parasite-induced mortality was significantly >50%: nine sites for *P. regilla* (5% of observed sites with *R. ondatrae* present), five sites for *T. torosa* (6% of sites), six sites for *A. boreas* (15% of sites) and zero sites for *T. granulosa* (Figure 4b). In addition, there were 11 total sites for *P. regilla*, *A. boreas* and *T. torosa* where median parasite-induced mortality was >90% (Figure 4b). However, parasite-induced mortality was only significantly >90% based on a 95% credible interval for two of these high mortality sites (one for *A. boreas* and one *P. regilla*). Sites with high parasite-induced mortality

were characterized by high pre-mortality mean parasite intensity μ and low levels of parasite aggregation (high k) relative to the species-level averages (Figure S3).

3.4 | Estimates of landscape-level parasite-induced mortality

Considering all sampled patches on the landscape, the total number of *P. regilla* hosts that suffered mortality within a year ranged from 20 to 200 hosts per 100 m² of littoral zone (Figure 5a). Total yearly median mortality per 100 m² for *A. boreas* was between 3 and 130 hosts and *T. torosa* was between 5 and 70 (Figure 5a). *T. granulosa* had the lowest predicted total mortality per 100 m², ranging from <1 to 7 hosts (Figure 5a).

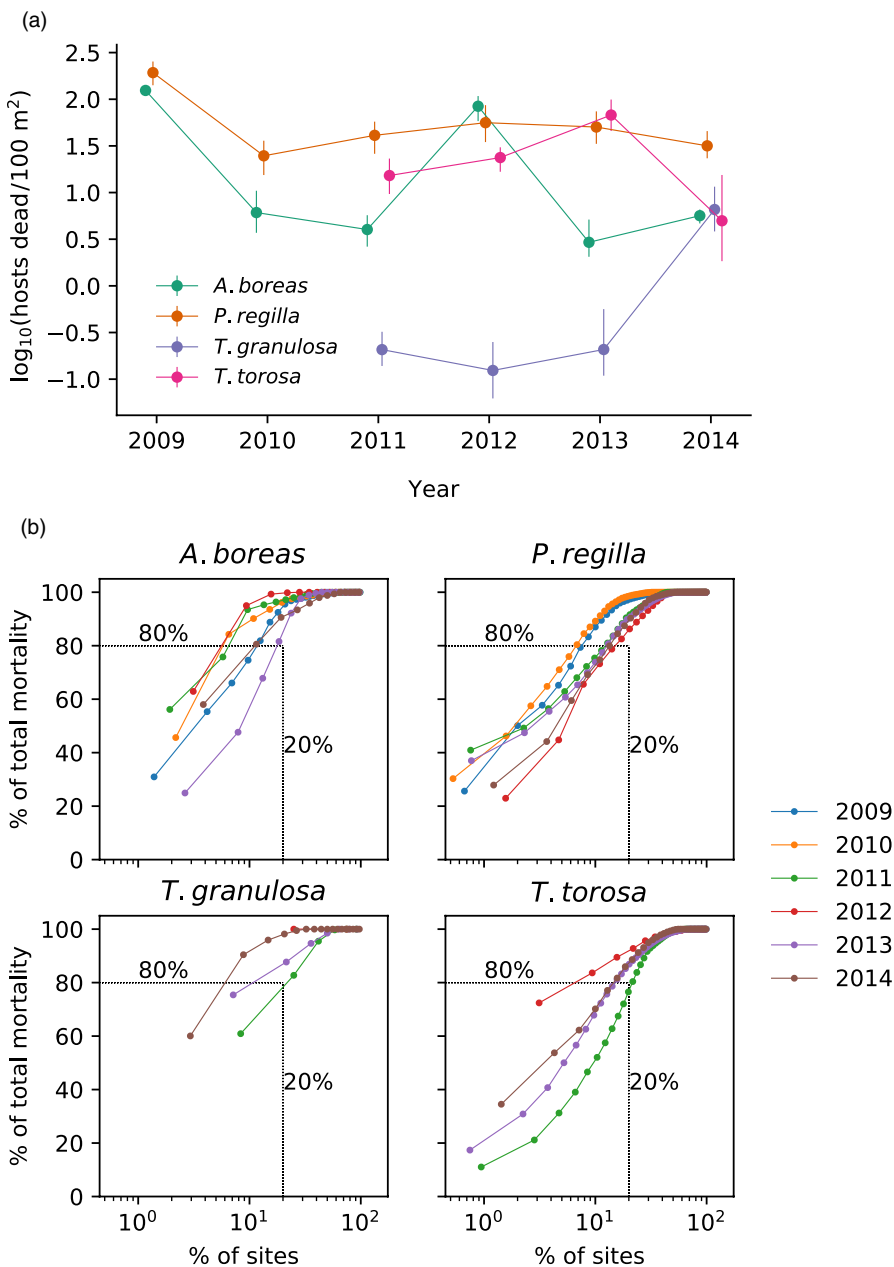


FIGURE 5 (a) The total estimated \log_{10} mortality per 100 m² of littoral zone for a given species across all sites with density estimates in a given year. The points are the median total mortality estimates and the error bars are the 95% credible intervals after propagating uncertainty in site-level parasite-induced mortality (Ω). We did not include total mortality estimates for *T. torosa* or *T. granulosa* in 2009 and 2010 as there were only two sites where hosts were dissected (Table S1). (b) The cumulative contribution of sites with non-zero host density to total predicted parasite-induced mortality for a given species within a given year. Sites were ranked based on total predicted host mortality and plotted in rank order, with the point to the farthest left on a curve being the site that contributed the most to total mortality on the landscape. In order to visualize the relative contributions of individual sites to total mortality on the landscape, (b) does not standardize total mortality by the area of the littoral zone at a site. Dotted lines are plotted for reference at 80% total mortality and 20% of observed sites

The predicted landscape-level patterns of mortality were largely driven by a few high mortality sites (Figure 5b). For a single site in a given year, the largest median predicted mortality was 3,853 individuals for *A. boreas* (95% CI for total mortality: [3,761, 3,871]; 95% CI for mortality per m²: [50, 52]), 4,890 for *P. regilla* (95% CI for total mortality: [3,674, 5,448]; 95% CI for mortality per m²: [12, 19]), 251 for *T. granulosa* (95% CI for total mortality: [117, 615]; 95% CI for mortality per m²: [1, 5]) and 1,100 for *T. torosa* (95% CI for total mortality: [964, 1,120]; 95% CI for mortality per m²: [4, 6]). For all species across all years, 20% of sites often contributed to 80% or more of the total mortality on the landscape (Figure 5b).

4 | DISCUSSION

Despite the ubiquity of parasite infections in wildlife, detecting and adequately quantifying the amount of parasite-induced mortality in a population is notoriously difficult. Linking dead or dying hosts—which are nearly impossible to detect in many natural systems—to a specific causal agent or pathogen is fraught with challenges surrounding observational bias, causal inference and interactions among stressors (McCallum, 2000). Outside the cases involving recently introduced pathogens or experimental manipulation, even coarse approximations of mortality associated with disease may be little more than guesswork. Here we combined experimental data, extensive field surveys and novel statistical models to estimate the amount of mortality induced by the virulent trematode parasite *R. ondatrae* within amphibian host communities across 301 populations and 6 years of surveys. At an average pond where the parasite was present, an estimated 13%–40% of larvae suffered *R. ondatrae*-induced mortality, depending on the amphibian species. Our models predicted that mortality was highly heterogeneous across populations, with >90% of hosts suffering parasite-induced mortality in some populations. Based on these high levels of mortality, our model predicted that in some ponds thousands of amphibian larvae succumbed to *R. ondatrae* infections. These estimates provide rare insight into the magnitude of the effects that macroparasites can have on host populations in the field.

A challenge with estimating population-level mortality using observational data is that it is inevitably difficult to validate estimates of parasite-induced mortality since one does not directly observe host mortality in the field. However, extensive knowledge of the biology of *R. ondatrae*–amphibian interactions and logical links between experimental and field data suggest three reasons the mortality estimates in this study are underestimates of *R. ondatrae*-induced amphibian mortality. First, in addition to amphibian larvae suffering intensity-dependent parasite mortality (which was the mortality we quantified in this study), infection acquired during the larval stage can lead to severe limb malformations in amphibian metamorphs, which reduce fitness and increase mortality risk (Goodman & Johnson, 2011; Johnson et al., 2002). In amphibian populations in our study area, the prevalence of limb malformation in metamorphs can be as high as 75% and a significant percentage of these

malformations have been robustly linked to *R. ondatrae* infection intensity through laboratory and mesocosm experiments (Johnson et al., 2012, 2013; McDevitt-Galles et al., 2020). It is therefore likely that the effects of *R. ondatrae* on amphibian mortality can extend beyond the larval stage. Second, our calculation of population-level mortality assumed that the survival of uninfected hosts was unaffected by *R. ondatrae*. However, laboratory experiments have shown that avoiding infection through mechanisms such as behavioural resistance comes at a cost (Sears et al., 2015). Thus, assuming that *R. ondatrae* has no effect on the survival of uninfected hosts ignores the costs that avoiding infection imposes on larval survival. Finally, the laboratory experiments we used to estimate dose-response curves between *R. ondatrae* infection and host survival inevitably ignored synergistic interactions between infection and the natural environment, and thus likely underestimated the effects of *R. ondatrae* infection on individual host survival (McCallum, 2000).

In contrast, the timing of *R. ondatrae* infection could lead to our mortality estimates being biased high. Previous studies have shown that the timing of trematode infection during larvae development can have significant effects on subsequent host mortality (Schotthoefer et al., 2003). The laboratory exposures used in this study involved a pulse infection event during early limb development, whereas hosts in natural systems could be exposed more continuously throughout larvae development. This would include a period both before limb growth (when hosts are even more vulnerable to parasite-induced mortality) as well as later in development when they are less vulnerable. This may help explain why our models for *A. boreas* and *T. granulosa* populations showed that there was often at least one host that we observed in a population that should have already succumbed to *R. ondatrae* mortality, given the observed parasite intensity and intensity-dependent mortality curves from the laboratory (Figure S4). While it is possible that these hosts were doomed to die and we simply sampled them before mortality—a situation we accounted for in our statistical model—it is also possible that heterogeneities in timing of infection meant that these individuals acquired *R. ondatrae* infection after the time when they were most vulnerable to succumbing to intensity-dependent parasite mortality (or that these individuals were inherently more tolerant of infection). While we were unable to account for these sources of individual heterogeneity in our mortality estimates, they are important factors to consider in future efforts for validating these predictions.

How does the predicted population-level mortality induced by *R. ondatrae* compare with the population-level effects of macroparasite infections in other wildlife hosts? The most direct comparisons come from the few other studies that have estimated parasite-induced mortality using a conceptually similar approach. Across six populations of the amphipod host *Gammarus pulex* infected with the acanthocephalan *Polymorphus minutus*, Crofton (1971) estimated between 0% and 22% of hosts were lost to parasite infection. For lizard fish infected with blastocysts of the cestode *Callitetrarhynchus gracilis*, Adjei et al. (1986) estimated mortality ranging from 2% to 11%. For Coho salmon infected with metacercariae of the digenean parasite *Apophallus* sp., Ferguson et al. (2011) predicted that 4% of hosts were lost to infection (inferred from table 2 in Ferguson

et al., 2011). The average mortality estimates from our study were qualitatively similar to these previous studies, though estimated *A. boreas* mortality was notably higher. To provide an even more direct comparison to *R. ondatrae*, we further estimated mortality induced by the trematode parasite *Echinostoma trivolvis*—also found in this system—on the amphibians *P. regilla* and *A. boreas* using an identical methodology to *R. ondatrae* (Appendix S3). We found that the average mortality estimates for both host species were 4% (*P. regilla* 95% CI: [3.0%, 6.1%]; *A. boreas* 95% CI: [1.8%, 14.1%]) and significantly lower than mortality estimates for *R. ondatrae* (Appendix S3). These estimated levels of mortality, were consistent with current hypotheses that *E. trivolvis* infection could have population-level effects on amphibians, but that these effects are likely less than *R. ondatrae* (Johnson & McKenzie, 2008).

An important advantage of our approach is that by using a likelihood framework we can quantify uncertainty in mortality estimates and extend the model to relax previously restrictive assumptions regarding the timing of parasite-induced mortality. While these advantages expand the number of host–parasite systems to which our approach can be applied, it is not applicable to all host–parasite systems. Particularly, our approach is currently limited to host–parasite systems where infection occurs over a specific time period in a host's life. There are, however, opportunities to extend our approach to other host–parasite systems with intensity-dependent mortality that do not meet this assumption. In host–parasite systems where parasites reproduce within a host, infection occurs continuously over a host's life, and hosts suffer intensity-dependent mortality (e.g. amphibians infected with chytrid fungus, Vredenburg et al., 2010), an interaction between variability in parasite growth among hosts and strong intensity-dependent mortality may leave a distinct mortality signature on observed parasite intensity distributions. In this case, our approach could potentially be extended to infer the magnitude of parasite-induced mortality from the observed distributional patterns (but see Duerr et al., 2003, for a cautionary tale).

Another contribution of this study is to illustrate how the combination of experimental data, field surveys and a robust likelihood-based approach facilitates inference into parasite-induced mortality across hundreds of populations of hosts, providing comprehensive estimates of not only average population-level mortality, but also variability in mortality across populations. Generally, epidemics in wildlife populations have provided the canonical examples of heterogeneity in population-level responses to an invading parasite (e.g. Frick et al., 2017; Wilber et al., 2019), but rarely have the population-level effects of endemic macroparasites been quantified for more than a few populations. For the four amphibian species in our system, *R. ondatrae* induced-mortality was highly heterogeneous across habitat patches, with generally fewer than 20% of sites contributing to more the 80% of the predicted total mortality across sites within a year. The factors that determine a mortality hotspot will depend on interactions among disease processes across scales, from the individual to the landscape (Paull et al., 2012). While an exploration of the mechanistic drivers of mortality hotspots was beyond the scope of this study, our analysis

did make two important observations relating to mortality hotspots for *R. ondatrae*.

First, infection intensity in larval amphibians is proportional to the exposure of amphibian larvae to *R. ondatrae* cercariae in the water, where cercariae density is related to infected planorbid snail density in the pond (Johnson & McKenzie, 2008). Therefore, an initial expectation would be that a mortality hotspot for one species would be a mortality hotspot for another species as both species are interacting with the pool of cercariae in the environment. Indeed, we found a significant correlation between the hotspots and cold spots of co-occurring species (Appendix S4, Figure S5). This result provides preliminary evidence that dominant factors mediating mortality hotspots may be exogenous to the host community, a hypothesis that we will explore in future studies. Second, we surprisingly saw only weak evidence that mortality hotspots were consistent through time, which we would have expected if pond characteristics that mediated exposure risk were temporally invariant (Appendix S4, Figure S5). Between-year fluctuations in the density of infected snails within a pond serve as a candidate mechanism driving the lack of temporal consistency in mortality hotspots.

An important challenge in wildlife health is understanding the extent to which parasites regulate and suppress host populations (Anderson & May, 1978; Tompkins et al., 2011). We cannot directly link the estimates of parasite-induced mortality we provide here with population regulation because we do not know the extent to which parasite-induced mortality is compensatory or additive (Kistner & Belovsky, 2014). For example, it is possible that amphibian larvae succumbing to parasite infection would have died from other causes in the absence of infection, such as predation. In this case, observed levels of *R. ondatrae*-induced mortality may have little effect on population dynamics. In contrast, if parasite-induced mortality is non-compensatory, then an important question from a conservation perspective is what level of parasite-induced mortality may result in amphibian population densities being reduced to a level of concern? Answering this question will depend on the life-history strategy of the amphibian (e.g. slow vs. fast life history) and where density-dependence is acting within the amphibian life cycle. Moreover, as many amphibian species persist within an interconnected network of habitat patches (Heard et al., 2012), as do the species in our system, amphibian dispersal from ponds of low parasite-induced mortality could potentially offset the effects of high mortality hotspots on amphibian populations. This remains an important future direction to explore.

ACKNOWLEDGEMENTS

We would like to thank D. Calhoun, T. McDevitt-Galles, T. Riepe and K. Leslie for efforts in field collection and sample processing. We thank East Bay Regional Parks Districts, East Bay Municipal Utility District, Santa Clara County Parks, Blue Oak Ranch Reserve, California State Parks, The Nature Conservancy, Open Space Authority and Mid-peninsula Open Space for allowing us land access. This work was supported by funding from the National Institutes of Health (NIGMS) Ecology of Infectious Disease program, R01GM109499

and R01GM135935, the National Science Foundation (1149308 and 1754171), the National Geographic Society and the David and Lucile Packard Foundation. Thanks to S. Weinstein for her artistic contribution.

AUTHORS' CONTRIBUTIONS

M.Q.W. and P.T.J.J. conceived of the analysis; M.Q.W. and C.J.B. developed the theoretical framework; P.T.J.J. collected and provided data; M.Q.W. wrote the first draft and all authors contributed to the conceptual development and revision of the study.

DATA AVAILABILITY STATEMENT

Data are available from the Dryad Digital Repository <https://doi.org/10.25349/D9SG75> (Wilber et al., 2020).

ORCID

Mark Q. Wilber  <https://orcid.org/0000-0002-8274-8025>

Cheryl J. Briggs  <https://orcid.org/0000-0001-8674-5385>

Pieter T. J. Johnson  <https://orcid.org/0000-0002-7997-5390>

REFERENCES

- Adjei, E. L., Barnes, A., & Lester, R. J. G. (1986). A method for estimating possible parasite-related host mortality, illustrated using data from *Callitetrarhynchus gracilis* (Cestoda: Trypanorhyncha) in lizardfish (*Saurida* spp.). *Parasitology*, *92*, 227–243.
- AmphibiaWeb. (2020). <https://amphibiaweb.org>. University of California, Berkeley.
- Anderson, R. M., & May, R. M. (1978). Regulation and stability of host-parasite interactions: I. Regulatory processes. *Journal of Animal Ecology*, *47*, 219–247.
- Barbour, A. D., & Pugliese, A. (2000). On the variance-to-mean ratio in models of parasite distributions. *Advances in Applied Probability*, *32*, 701–719.
- Blehert, D. S., Hicks, A. C., Behr, M., Meteyer, C. U., Berlowski-Zier, B. M., Buckles, E. L., Coleman, J. T. H., Darling, S. R., Gargas, A., Niver, R., Okoniewski, J. C., Rudd, R. J., & Ward, B. (2008). Bat white-nose syndrome: An emerging fungal pathogen? *Science*, *323*, 227. <https://doi.org/10.1126/science.1163874>
- Crofton, H. D. (1971). A quantitative approach to parasitism. *Parasitology*, *62*, 179–193. <https://doi.org/10.1017/S0031182000071420>
- Dobson, A. P., & Hudson, P. J. (1992). Regulation and stability of a free-living host-parasite system: *Trichostrongylus tenuis* in red grouse. II. Population models. *Journal of Animal Ecology*, *61*, 487–498. <https://doi.org/10.2307/5339>
- Duerr, H. P., Dietz, K., & Eichner, M. (2003). On the interpretation of age-intensity profiles and dispersion patterns in parasitological surveys. *Parasitology*, *126*, 87–101. <https://doi.org/10.1017/S0031182002002561>
- Fereidouni, S., Freimanis, G. L., Orynbayev, M., Ribeca, P., Flannery, J., King, D. P., Zuther, S., Beer, M., Höper, D., Kydyrmanov, A., Karamendin, K., & Kock, R. (2019). Mass die-off of saiga antelopes, Kazakhstan, 2015. *Emerging Infectious Diseases*, *25*, 1169–1176. <https://doi.org/10.3201/eid2506.180990>
- Ferguson, J. A., Koketsu, W., Ninomiya, I., Rossignol, P. A., Jacobson, K. C., & Kent, M. L. (2011). Mortality of Coho salmon (*Oncorhynchus kisutch*) associated with burdens of multiple parasite species. *International Journal for Parasitology*, *41*, 1197–1205. <https://doi.org/10.1016/j.ijpara.2011.07.005>
- Fisher, M. C., Henk, D. A., Briggs, C. J., Brownstein, J. S., Madoff, L. C., McCraw, S. L., & Gurr, S. J. (2012). Emerging fungal threats to animal, plant and ecosystem health. *Nature*, *484*, 186–194. <https://doi.org/10.1038/nature10947>
- Frick, W. F., Cheng, T. L., Langwig, K. E., Hoyt, J. R., Janicki, A. F., Parise, K. L., Foster, J. T., & Kilpatrick, A. (2017). Pathogen dynamics during invasion and establishment of white-nose syndrome explain mechanisms of host persistence. *Ecology*, *98*, 624–631. <https://doi.org/10.1002/ecy.1706>
- Goodman, B. A., & Johnson, P. T. J. (2011). Disease and the extended phenotype: Parasites control host performance and survival through induced changes in body plan. *PLoS One*, *6*, e20193. <https://doi.org/10.1371/journal.pone.0020193>
- Gosner, K. L. (1960). A simplified table for staging anuran embryos and larvae with notes on identification. *Herpetologica*, *16*, 183–190.
- Hartson, R. B., Orlofske, S. A., Melin, V. E., Dillon, R. T., & Johnson, P. T. J. (2011). Land use and wetland spatial position jointly determine amphibian parasite communities. *EcoHealth*, *8*, 485–500. <https://doi.org/10.1007/s10393-011-0715-9>
- Hayward, A. D., Garnier, R., Childs, D. Z., Grenfell, B. T., Watt, K. A., Pilkington, J. G., Pemberton, J. M., & Graham, A. L. (2019). From population to individual host scale and back again: Testing theories of infection and defence in the Soay sheep of St Kilda. In K. R. Wilson, A. Fenton, & D. M. Tompkins (Eds.), *Wildlife conservation in a changing climate* (pp. 91–128). Cambridge University Press.
- Heard, G. W., Scroggie, M. P., & Malone, B. S. (2012). Classical metapopulation theory as a useful paradigm for the conservation of an endangered amphibian. *Biological Conservation*, *148*, 156–166. <https://doi.org/10.1016/j.biocon.2012.01.018>
- Hudson, P. J., Dobson, A. P., & Newborn, D. (1998). Prevention of population cycles by parasite removal. *Science*, *282*, 2256–2258. <https://doi.org/10.1126/science.282.5397.2256>
- Johnson, P. T. J., & Hoverman, J. T. (2012). Parasite diversity and coinfection determine pathogen infection success and host fitness. *Proceedings of the National Academy of Sciences of the United States of America*, *109*, 9006–9011. <https://doi.org/10.1073/pnas.1201790109>
- Johnson, P. T. J., Longcore, J. E., Stanton, D. E., Carnegie, R. B., Shields, J. D., & Preu, E. R. (2006). Chytrid infections of *Daphnia pulex*: Development, ecology, pathology and phylogeny of *Polycaryum laeve*. *Freshwater Biology*, *51*, 634–648. <https://doi.org/10.1111/j.1365-2427.2006.01517.x>
- Johnson, P. T. J., Lunde, K. B., Thurman, E. M., Ritchie, E. G., Wray, S. N., Sutherland, D. R., Kapfer, J. M., Frest, T. J., Bowerman, J., & Blaustein, A. R. (2002). Parasite (*Ribeiroia ondatrae*) infection linked to amphibian malformations in the Western United States. *Ecological Monographs*, *72*, 151–168. [https://doi.org/10.1890/0012-9615\(2002\)072\[0151:PROILT\]2.0.CO;2](https://doi.org/10.1890/0012-9615(2002)072[0151:PROILT]2.0.CO;2)
- Johnson, P. T. J., & McKenzie, V. J. (2008). Effects of environmental change on helminth infections in amphibians: Exploring the emergence of *Ribeiroia* and *Echinostoma* infections in North America. In B. Fried & R. Toledo (Eds.) *The biology of echinostomes* (chap. 11, pp. 249–280). Springer Science+Business Media.
- Johnson, P. T. J., Preston, D. L., Hoverman, J. T., & Richgels, K. L. D. (2013). Biodiversity decreases disease through predictable changes in host community competence. *Nature*, *494*, 230–233. <https://doi.org/10.1038/nature11883>
- Johnson, P. T. J., Rohr, J. R., Hoverman, J. T., Kellermanns, E., Bowerman, J., & Lunde, K. B. (2012). Living fast and dying of infection: Host life history drives interspecific variation in infection and disease risk. *Ecology Letters*, *15*, 235–242. <https://doi.org/10.1111/j.1461-0248.2011.01730.x>
- Johnson, P. T. J., & Wilber, M. Q. (2017). Biological and statistical processes jointly drive population aggregation: Using host – parasite interactions to understand Taylor's power law. *Proceedings of the Royal Society B: Biological Sciences*, *284*, 20171388. <https://doi.org/10.1098/rspb.2017.1388>

- Johnson, P. T. J., Wood, C. L., Joseph, M. B., Preston, D. L., Haas, S. E., & Springer, Y. P. (2016). Habitat heterogeneity drives the host-diversity-begets-parasite-diversity relationship: Evidence from experimental and field studies. *Ecology Letters*, 19, 752–761. <https://doi.org/10.1111/ele.12609>
- Jones, K. E., Patel, N. G., Levy, M. A., Storeygard, A., Balk, D., Gittleman, J. L., & Daszak, P. (2008). Global trends in emerging infectious diseases. *Nature*, 451, 990–993. <https://doi.org/10.1038/nature06536>
- Kistner, E., & Belovsky, G. E. (2014). Host dynamics determine responses to disease: Additive vs. compensatory mortality in a grasshopper-pathogen system. *Ecology*, 95, 2579–2588. <https://doi.org/10.1890/13-0969.1>
- Krkošek, M., Morton, A., Volpe, J. P., & Lewis, M. A. (2009). Sea lice and salmon population dynamics: Effects of exposure time for migratory fish. *Proceedings of the Royal Society B: Biological Sciences*, 276, 2819–2828.
- Lafferty, K. D., & Kuris, A. M. (2002). Trophic strategies, animal diversity and body size. *Trends in Ecology & Evolution*, 17, 507–513. [https://doi.org/10.1016/S0169-5347\(02\)02615-0](https://doi.org/10.1016/S0169-5347(02)02615-0)
- Lafferty, K. D., & Morris, A. K. (1996). Altered behavior of parasitized killifish increases susceptibility to predation by bird final hosts. *Ecology*, 77, 1390–1397. <https://doi.org/10.2307/2265536>
- McCallum, H. I. (2000). Host-pathogen and host-parasite models. In J. H. Lawton & G. E. Likens (Eds.), *Population parameters: Estimation for ecological models* (chap. 10, pp. 284–312). Blackwell Science Ltd.
- McCallum, H. (2012). Disease and the dynamics of extinction. *Philosophical Transactions of the Royal Society B: Biological Sciences*, 367, 2828–2839. <https://doi.org/10.1098/rstb.2012.0224>
- McCallum, H., Jones, M., Hawkins, C., Hamede, R., Lachish, S., Sinn, D. L., Beeton, N., & Lazenby, B. (2009). Transmission dynamics of Tasmanian devil facial tumor disease may lead to disease-induced extinction. *Ecology*, 90, 3379–3392. <https://doi.org/10.1890/08-1763.1>
- McDevitt-Galles, T., Moss, W. E., Calhoun, D. M., & Johnson, P. T. J. (2020). Phenological synchrony shapes pathology in host-parasite systems. *Proceedings of the Royal Society B: Biological Sciences*, 287, 20192597. <https://doi.org/10.1098/rspb.2019.2597>
- Murdoch, W., Briggs, C. J., & Swarbrick, S. (2005). Ecology: Host suppression and stability in a parasitoid-host system: Experimental demonstration. *Science*, 309, 610–613. <https://doi.org/10.1126/science.1114426>
- Paull, S. H., Song, S., McClure, K. M., Sackett, L. C., Kilpatrick, A. M., & Johnson, P. T. J. (2012). From superspreaders to disease hotspots: Linking transmission across hosts and space. *Frontiers in Ecology and the Environment*, 10, 75–82. <https://doi.org/10.1890/110111>
- Pielou, E. C. (1969). *An introduction to mathematical ecology*. New York, NY: John Wiley & Sons Ltd.
- Pontoppidan, M. B., Himaman, W., Hywel-Jones, N. L., Boomsma, J. J., & Hughes, D. P. (2009). Graveyards on the move: The spatio-temporal distribution of dead ophiocordyceps-infected ants. *PLoS One*, 4, e4835. <https://doi.org/10.1371/journal.pone.0004835>
- Poulin, R. (2007). Are there general laws in parasite ecology? *Parasitology*, 134, 763–776. <https://doi.org/10.1017/S0031182006002150>
- Poulin, R., & Morand, S. (2000). The diversity of parasites. *The Quarterly Review of Biology*, 75, 277–293. <https://doi.org/10.1086/393500>
- Richgels, K. L. D., Hoverman, J. T., & Johnson, P. T. J. (2013). Evaluating the role of regional and local processes in structuring a larval trematode metacommunity of *Helisoma trivolvis*. *Ecography*, 36, 854–863.
- Salvatier, J., Wiecki, T. V., & Fonnesbeck, C. (2016). Probabilistic programming in Python using PyMC3. *PeerJ Computer Science*, 2, e55. <https://doi.org/10.7717/peerj-cs.55>
- Scheele, B. C., Pasmans, F., Skerratt, L. F., Berger, L., Martel, A. N., Beukema, W., Acevedo, A. A., Burrowes, P. A., Carvalho, T., Catenazzi, A., De la Riva, I., Fisher, M. C., Flechas, S. V., Foster, C. N., Frías-Álvarez, P., Garner, T. W. J., Gratwicke, B., Guayasamin, J. M., Hirschfeld, M., & Canessa, S. (2019). Amphibian fungal panzootic causes catastrophic and ongoing loss of biodiversity. *Science*, 363, 1459–1463. <https://doi.org/10.1126/science.aav0379>
- Schotthoefer, A. M., Cole, R. A., & Beasley, V. R. (2003). Relationship of tadpole stage to location of echinostome cercariae encystment and the consequences for tadpole survival. *The Journal of Parasitology*, 89, 475–482. [https://doi.org/10.1645/0022-3395\(2003\)089\[0475:ROTSTL\]2.0.CO;2](https://doi.org/10.1645/0022-3395(2003)089[0475:ROTSTL]2.0.CO;2)
- Scott, M. E. (1988). The impact of infection and disease on animal populations: Implications for conservation biology. *Conservation Biology*, 2, 40–56. <https://doi.org/10.1111/j.1523-1739.1988.tb00334.x>
- Sears, B. F., Snyder, P. W., & Rohr, J. R. (2015). Host life history and host-parasite syntopy predict behavioural resistance and tolerance of parasites. *Journal of Animal Ecology*, 84, 625–636. <https://doi.org/10.1111/1365-2656.12333>
- Shaw, D. J., Grenfell, B. T., & Dobson, A. P. (1998). Patterns of macroparasite aggregation in wildlife host populations. *Parasitology*, 117, 597–610. <https://doi.org/10.1017/S0031182098003448>
- Tompkins, D. M., Carver, S., Jones, M. E., Krkošek, M., & Skerratt, L. F. (2015). Emerging infectious diseases of wildlife: A critical perspective. *Trends in Parasitology*, 31, 149–159. <https://doi.org/10.1016/j.pt.2015.01.007>
- Tompkins, D. M., Dunn, A. M., Smith, M. J., & Telfer, S. (2011). Wildlife diseases: From individuals to ecosystems. *Journal of Animal Ecology*, 80, 19–38. <https://doi.org/10.1111/j.1365-2656.2010.01742.x>
- Vredenburg, V. T., Knapp, R. A., Tunstall, T. S., & Briggs, C. J. (2010). Dynamics of an emerging disease drive large-scale amphibian population extinctions. *Proceedings of the National Academy of Sciences of the United States of America*, 107, 9689–9694. <https://doi.org/10.1073/pnas.0914111107>
- Watson, M. J. (2013). What drives population-level effects of parasites? Meta-analysis meets life-history. *International Journal for Parasitology: Parasites and Wildlife*, 2, 190–196.
- Wilber, M. Q., Briggs, C. J., & Johnson, P. T. J. (2020). Data from: Disease's hidden death toll: Using parasite aggregation patterns to quantify landscape-level host mortality in a wildlife system. *Dryad Digital Repository*, <https://doi.org/10.25349/D9SG75>
- Wilber, M. Q., Johnson, P. T. J., & Briggs, C. J. (2019). When chytrid fungus invades: Integrating theory and data to understand disease-induced amphibian declines. In K. Wilson, A. Fenton & D. M. Tompkins (Eds.), *Wildlife disease ecology: Linking theory to data and application* (pp. 511–543). Cambridge University Press.
- Wilber, M. Q., Weinstein, S. B., & Briggs, C. J. (2016). Detecting and quantifying parasite-induced host mortality from intensity data: Method comparisons and limitations. *International Journal for Parasitology*, 46, 59–66. <https://doi.org/10.1016/j.ijpara.2015.08.009>
- Wong, C. J., & Liversage, R. A. (2005). Limb developmental stages of the newt *Notophthalmus viridescens*. *International Journal for Developmental Biology*, 389, 375–389. <https://doi.org/10.1387/ijdb.041910cw>
- World Health Organization. (2018). *Global Health Observatory Data: Top ten causes of death*. World Health Organization. Retrieved from <https://www.who.int/data/gho/data/themes/topics/causes-of-death/GHO/causes-of-death>

SUPPORTING INFORMATION

Additional supporting information may be found online in the Supporting Information section.

How to cite this article: Wilber MQ, Briggs CJ, Johnson PTJ.

Disease's hidden death toll: Using parasite aggregation patterns to quantify landscape-level host mortality in a wildlife system. *J. Anim. Ecol.* 2020;00:1–12. <https://doi.org/10.1111/1365-2656.13343>